Accurate determination of optical parameters of non transparent materials: the ϵ–GaSe case

A. Bassou, A. Rajira, B. Gil, A. Almaggoussi, A. Abounadi

Accurate determination of optical parameters of non transparent materials: the ε–GaSe case

A. Bassou[a], A. Rajira[a*], B. Gil[b], A. Almaggoussi[a], A. Abounadi[a]

[a]IMED-Lab, Université Cadi Ayyad, Faculté des Sciences et Techniques, BP 549, 40000 Marrakech, Morocco

[b]Laboratoire Charles Coulomb, UMR 5221 CNRS, Université de Montpellier, 34095 Montpellier, France

Abstract

This work reports on the modeling and precise determination of the optical parameters of mechanically exfoliated gallium selenide (ε–GaSe) thin films from both measured transmittance (T_{meas}) and reflectance (R_{meas}) at room temperature. Then, the absorption $\alpha(\lambda)$ and the reflection $R(\lambda)$ coefficients were accurately calculated, at any wavelength. More general relations taking into account the multiple transmissions and the multiple reflections on both sides of the ε–GaSe film were considered. The fundamental optical constants that are the complex refractive index $N(\lambda)$ and the complex dielectric constant $\varepsilon(\lambda)$ were then accurately determined. Modeling the imaginary part of the latter parameter permits a precise determination of the positions of the resonances observed in the transmittance and reflectance spectra. The modeling was handled by considering an increasing number from three to five oscillators within the Lorentz model. The assignation of these resonances to the related critical points of the Brillouin zone at and above the band gap was investigated. The splitting on the valence band and the close indirect-direct nature of the configuration in the conduction band have been considered simultaneously. For GaSe material, the refractive index varies from 2.8 and 3.3 with strong peaks above the band gap corresponding to resonances at 3.2 eV and 3.7 eV. The analysis of the oscillator strengths and the lifetimes of the observed transitions allowed to clearly identifying the indirect nature of the fundamental band gap. Its value of 1.97 eV is largely separated from the direct band gap of about 230 meV. The transition lifetimes were found to vary between 0.6 fs and 24 fs.

Keywords: Gallium Selenide exfoliation; Reflectance and transmittance; Optical constants; Complex dielectric constant; Lorentz model; Resonance frequencies.

*** Corresponding author**: Phone: (+212) 524433404 / 3163 / Fax: (+212) 524433170

E-mail: a.rajira@uca.ma

1. Introduction

GaSe is a lamellar III-VI semiconductor that crystallizes in 4 different layered structures, β, γ, δ and ε [1]. Among these polytypes, ε–GaSe has current optical applications, including photodetectors [2-4], phototransistors [5,6], energy storage [7] and non linear optical devices [8-10]. Besides, its band gap can be tuned, either through an applied strain [11-14] or by reducing its thickness down to few layers [15,16], offering the opportunity for new devices design [11,17].

It is well known that complex refractive index is used to describe the dispersive nature of samples as well as their absorption properties. Thus, the chalcogenides materials like GaSe, having large non-linear responses and a high real refractive index are used in non-resonant devices [18]. Additionally, GaSe can be used as a light absorber in photovoltaic cells owing to its high absorption coefficient. Therefore, it is very convenient to study the optical parameters of GaSe since these parameters control the quality of the optical coupling between light and absorber. Furthermore, ε–GaSe can combine with other two-dimensional materials for ultrathin multifunctional devices [19, 20] based on the related heterojunctions properties.

The optical and electronic behaviour of a material can be understood through the knowledge of parameters such as refractive index n, extinction coefficient k, absorption coefficient α, as well as the band structure. An accurate determination of the wavelength dependence of the complex refractive index $N(\lambda)$ and of the complex dielectric constant $\varepsilon(\lambda)$ is then necessary to have important information on the material's optical features with the perspective of the realization of optoelectronic devices [21,22]. These two fundamental optical parameters depend not only on the absorption coefficient $\alpha(\lambda)$ but also on the reflection coefficient $R(\lambda)$ whose determination is somewhat controversial. Indeed, the most used formulas are available in the transparency range [23-27] rather than in the whole range which may lead to some inaccuracy in the optical parameters determination and thus in the interpretation of the experimental results.

In this work, we present a new and more accurate procedure for determining fundamental optical constants, across the entire studied wavelength range. This method is based on the simultaneous measurement of transmission and reflection spectra. The absorption and reflection coefficients were first determined by solving a 2-equation system, and then the other fundamental optical parameters were deduced. The Lorentz model of interband oscillators was applied for modeling the complex dielectric constant in order to determine the optical characteristics of the observed resonances in the experimental spectra. As an application example, we have chosen the ε–GaSe material. Indeed, this material is particularly known for its strong anisotropy and the proximity of its indirect and direct

band gaps [12,28,29]. In addition, despite a rich literature, there is a wide scatter of band structure parameter values [30-34].

The steps of the methodology, applied here in particular to the ε–GaSe material, are explained in Fig.1.

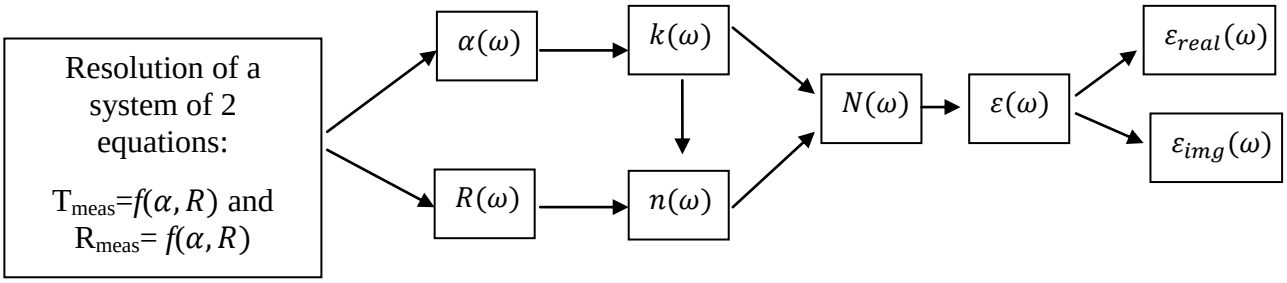

Fig.1: The steps, based on the simultaneous measurements of the transmittance and reflectance, which are followed for an accurate determination of fundamental optical constants.

2. Experimental

Bulk GaSe was purchased from HG Grahpene Company (KVK 59652233) with high purity (99.99%) [35]. Mechanical exfoliation from bulk GaSe was used to deposit GaSe on a transparent and flexible substrate (PolyEthylene Terephthalate PET). The peeling was repeated three times in order to separate a few sheets. No other treatment was performed. Optical measurements, transmittance and reflectance, were carried out in nearly normal incidence within the 250-1000 nm spectral range at room temperature using a dual beam computer-controlled UV–Visible–NIR spectrophotometer "UV-310PC-SHIMADZU".

3. Results and discussion

Detailed structural and morphological studies of the studied sample were presented in our previous works [12,36]. The Gase material was identified to be of ε-polytype, through the investigation of its structural, morphological and Raman properties.

In this work, the optical characterization is based not only on one optical measurement but on that of both the transmittance (T_{meas}) and the reflectance (R_{meas}). The spectra recorded at room temperature by using the same UV-VIS-IR spectrophotometer are presented in Fig. 2 in the range of [220 nm – 800 nm].

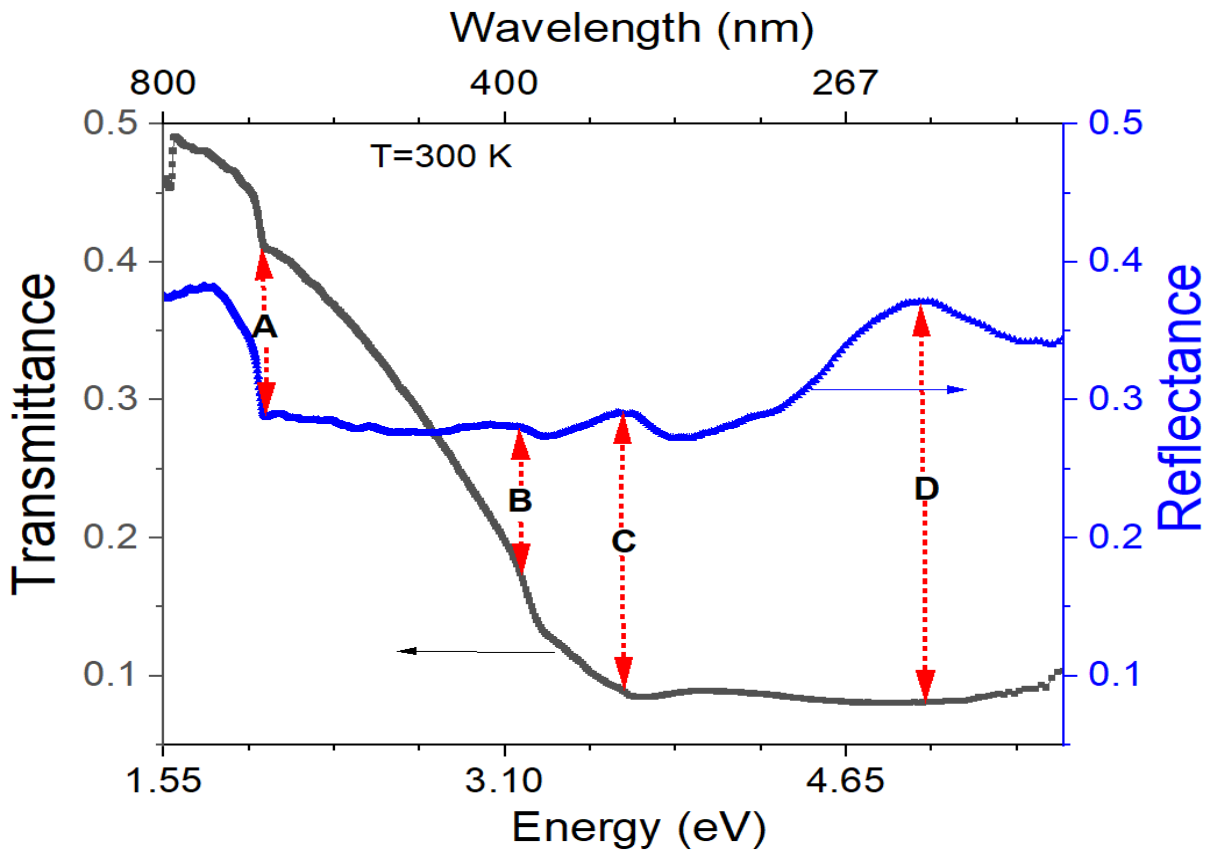

Fig. 2: Room temperature transmittance (T_{meas}) and reflectance (R_{meas}) spectra of the exfoliated GaSe thin film.

As can be seen in Fig.2, the transmittance reaches its maximum of about 50%, in the region of transparency. It decreases to less than 10% for energies well above the band gap. The reflectance, ranging between 25 and 38%, shows a regular behaviour with clear features related to the strong absorptions that occur at the critical points of the Brillouin zone (BZ). It is very interesting to note that the corresponding resonances, (A) at the edge of the band gap and (B, C, D) far above in energy, have the same positions in both spectra. The values of the energy position of each resonance, roughly determined from the spectra, are reported in Table 1. In this table are also reported values from literature and the corresponding assignation [37-41].

Table 1: The energy position of the resonances of our sample compared to those of the literature.

Resonance	Energy (wavelength) Our results	Literature values		
		[38]	[40]	[41]
A *(s-p_z)*	2.006eV (618nm)	~2.02ev	~2 eV	
B *(s-p_x)*	3.18eV (390nm)	~3.22eV	~3.2eV	
C *(s-p_y)*	3.65eV (339nm)	~3.64eV	~3.7eV	
D (Ga_2O_3)	4.96V (250nm)			~5.00eV

The assignation of A, B and C resonances is based on recent enhanced first principles calculations of the ε-GaSe band structure. There is an agreement regarding the valence band (VB) nature which is splitted due to both the high anisotropy degree and the spin-orbit interaction in this 2 dimensional material. The VB maxima, which are located at Γ point and whose main origin is from the p(Se) atomic orbitals, are P_z, P_x and P_y as represented in Fig.3. In this figure, S_d and S_i represent the conduction band (CB) minima respectively for direct and indirect band gaps.

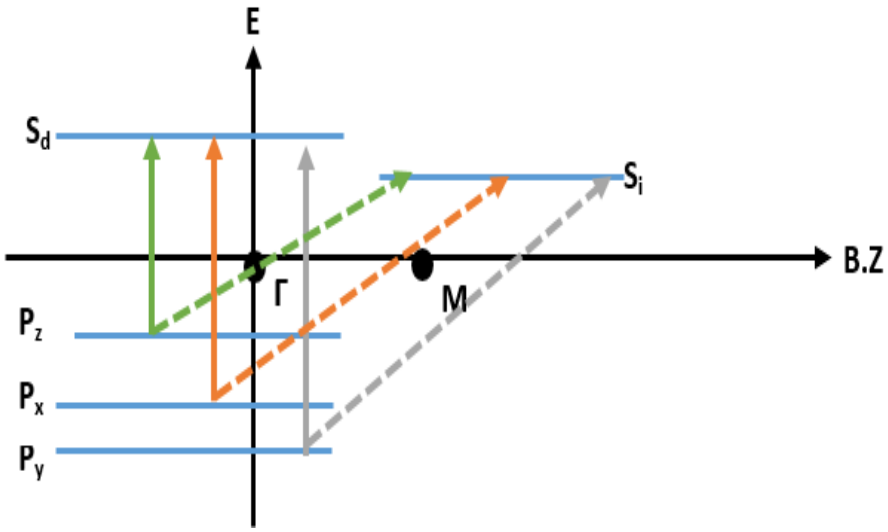

Fig. 3: Transitions from the states of the splitted VB to the indirect-direct CB states.

If there is also an agreement on the lowest conduction band (CB) origin, related mainly to s(Ga) atomic orbital, and on the closeness of the energy minima at Γ(S_d) and M(S_i) points, there is however a discrepancy on the nature of the fundamental band gap.

Besides the precise determination of optical constants of ε-GaSe, one of the main objectives of this article is to contribute to elucidate this problem. This will be done through the modeling of the

imaginary part of the dielectric constant which is determined with great accuracy from not only one optical measure but from two complementary, T_{meas} and R_{meas}, measurements [42,43]. This leads to the precise determination of the characteristics of all the resonances observed and hence to their assignation.

The resonance D at λ = 250 nm can be attributed to Ga_2O_3 since it coincides with its band gap energy. In fact, the existence of this phase is quite possible if we consider the photo-induced oxidation of GaSe layers. This resonance is strong in R(λ) because it results from the oxidation of the surface where the penetration of light is moderate due to the large value of the absorption at 4.96 eV, which is of a direct nature [41].

3.1 Optical constants determination as a function of wavelength

The transmittance and reflectance result from the multiple transmissions and the multiple reflections on both sides of a thin film. They are then expressed as a function of the reflection coefficient R (between air and the material), the absorption coefficient α and the thickness *d* of the media as follows [27,44,45]:

$$T_{meas} = \frac{(1-R)^2 e^{-\alpha d}}{1-R^2 e^{-2\alpha d}} \qquad (1)$$

$$R_{meas} = \frac{R+R(1-2R)e^{-2\alpha d}}{1-R^2 e^{-2\alpha d}} \qquad (2)$$

It can be seen that the precise determination of the absorption coefficient (and at the same time the reflection coefficient) requires not one but two optical measures.

The measurement of both T_{meas} and R_{meas} makes it possible to solve these two equations, forming a system of the two unknown, R and α, and leads to their determination at any wavelength of the whole considered range. As it is a non linear system, it can't be solved in a straight forward way, but through numerical resolution.

Here lets emphasize that the most commonly used equation for the determination of the absorption coefficient, $\alpha = \frac{1}{d}\ln\left(\frac{1}{T}\right)$, is a limit of equation (1) when R can be considered as small enough compared to 1, which means only in the transparency domain of well transparent materials. However, a material can have a significant variation in the magnitude of R which must be taken into account for understanding the optical behavior in an extended wavelength domain. It is the case of the GaSe material, where R has non-negligible values, of the order of 30 to 40% in the considered wavelength range, as can be seen in Fig. 2. Thus, a global determination of both its absorption and reflection coefficients, from equations 1 and 2, is necessary.

The absorption and reflection coefficients of our sample were determined from the numerical resolution. Their variations, in the energy range between 1.8 eV and 4 eV, are reported in Fig.4.

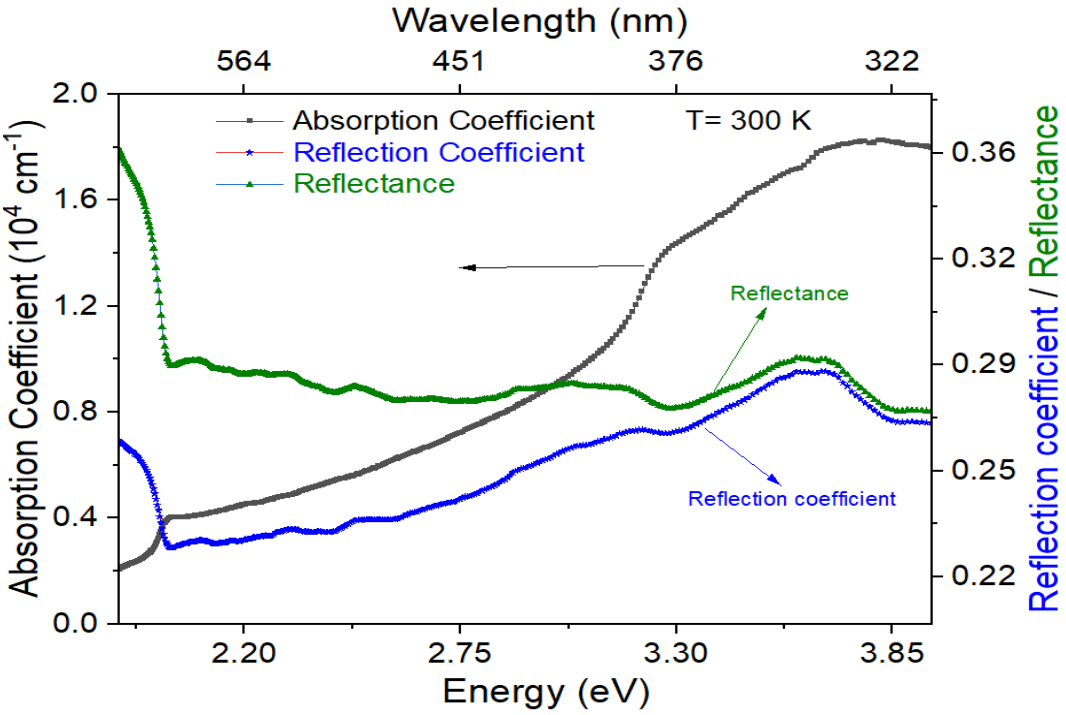

Fig. 4: The calculated optical absorption and reflection coefficients, as well as the measured reflectance, of the ε–GaSe sample as a function of the photon energy.

Figure 4 shows a clear edge starting at ~ 2 eV (620 nm) and beyond which the absorption increases strongly, reaching a value as high as 10^4 cm^{-1} and well defined features that correspond to resonant absorption at critical points. Note that the variation of the reflection coefficient, R, is quite different from that of the measured reflectance R_{meas}. The same tendency as a function of energy was obtained by Look and Leach [45] on GaN material.

Through the considered experimental and numerical processes, the other main optical parameters can also be accurately determined. Indeed, the components of the complex refractive index, $N(\lambda) = n(\lambda) + ik(\lambda)$, namely the refractive index n and the extinction coefficient k, at normal incidence, are respectively given by [46, 47]:

$$n = \frac{(R+1)+\sqrt{4R-(R-1)^2k^2}}{(1-R)} \qquad (3)$$

$$k = \frac{\alpha\lambda}{4\pi} \qquad (4)$$

The variation of these parameters as a function of energy is represented in Fig.5.

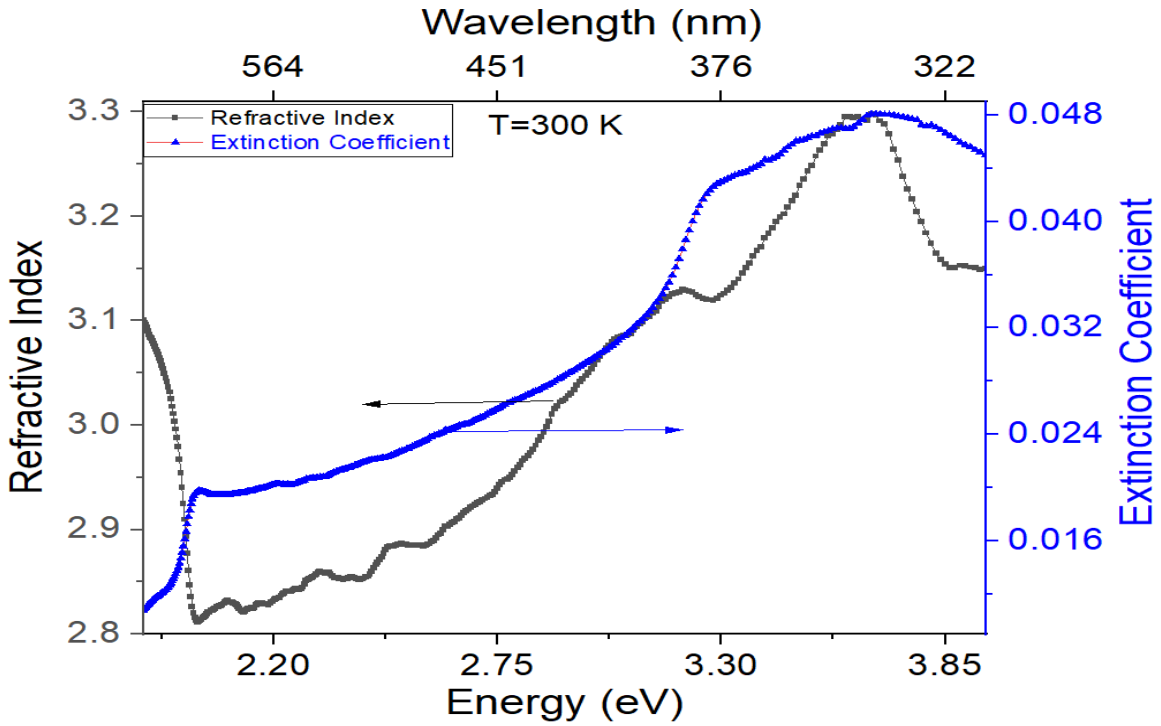

Fig. 5: ε–GaSe real refractive index *n* and extinction coefficient *k* versus photon energy.

The refractive index varies between 2.8 and 3.3 for the energy range 1.8 eV – 4 eV. These values are very close to those determined by other experimental methods, [22,48-50]. In particular, Kepinska et al [22] investigated both the ordinary $n_{\perp}$ and the extraordinary $n_{\parallel}$ real refractive indexes by a spectrogoniometric experimental method (through optical transmission spectra presenting interferential patterns). For the normal incidence the values measured for $n_{\perp}$ increased from 2.8 to 3.1 when increasing the energy from 1.24 eV to 2.48 eV with a peak at 1.99 eV which coincides with the resonant absorption at the bang gap's critical point. The same tendency was found for $n_{\parallel}$ but with lower values ranging between 2.6 and 2.85 for the same energy domain. Adachi et al [48], using ellipsometry, investigated a larger energy domain between 1.5 eV to 5 eV and found values of n increasing from 2.7 to 4 with strong resonances far above the band gap belonging to critical points of higher energies. We also observe strong peaks of *n* above the band gap corresponding to resonances at 3.2 eV and 3.7 eV.

A major consequence of the precise determination of the complex refractive index $N(\lambda)$, (resulting from that of the last two parameters) is the accurate determination of the complex dielectric function, $\varepsilon(\lambda) = \varepsilon_{real} + i\varepsilon_{img} = N^2(\lambda)$, through the whole wavelength range. The wavelength dependence of

the real ε_{real} and the imaginary ε_{img} parts of the complex dielectric constant, whose expressions are given by equations (5) and (6), are reported in Fig.6.

$$\varepsilon_{real} = n^2 - k^2 \qquad (5)$$

$$\varepsilon_{img} = 2\,nk \qquad (6)$$

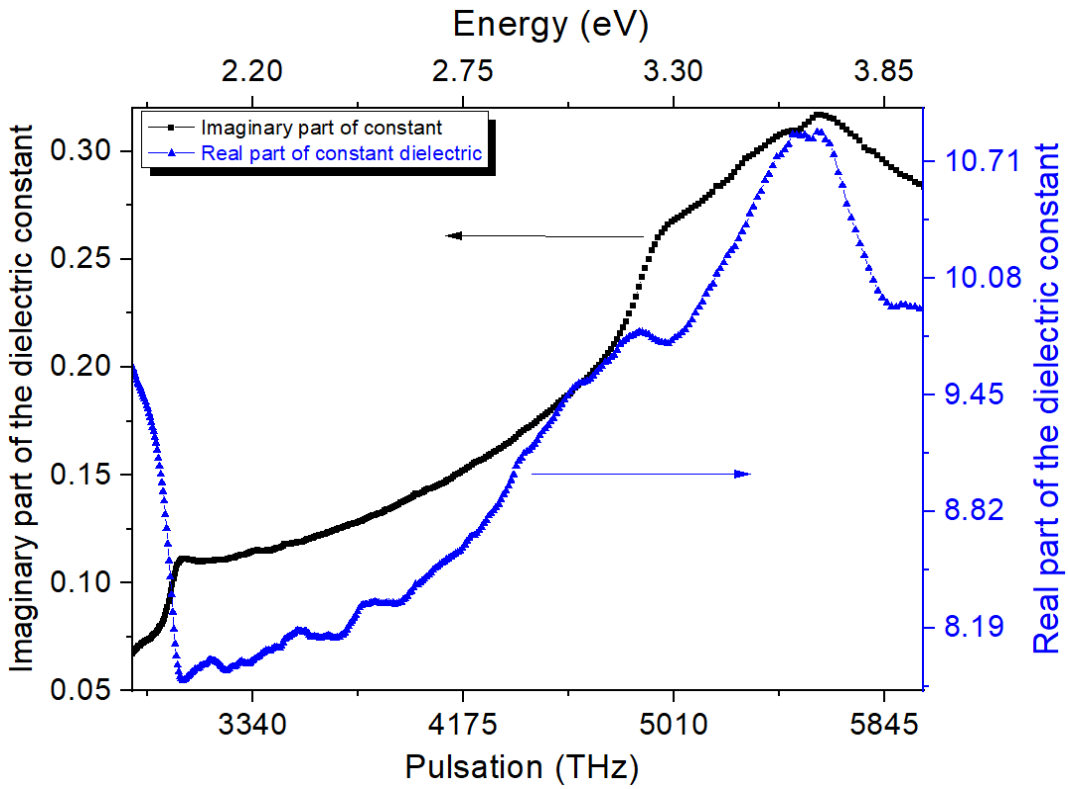

Fig 6: Pulsation dependence of the imaginary and real parts of the dielectric constant of ε–GaSe.

As the imaginary part of the dielectric constant behaves like the absorbance [51-53], it reveals complementary interesting information about the resonances related to the critical points. Its modeling would then makes it possible to precisely determine the energy position of each resonance observed on the optical spectra and would then help to assign the associated transition with respect to the GaSe band structure.

The modeling offers detailed information on each resonance characteristics, particularly its position and magnitude as well as the transition's life time. The first is linked to a specific critical point in the band structure, the second is related to the oscillator strength through the density of the electrons involved in the resonance while the last can be estimated through the determination of the transition's damping parameter.

3.2 Modeling the imaginary part, ε_{img}, of the complex dielectric constant

3.2.1 Formulas setting up

The modeling of $\varepsilon_{img}(\lambda)$ is done within the interband optical theory of dielectrics. We consider in particular Lorentz model which can be extended to the quantum approach. Indeed, the classical response of an electronic oscillator can be replaced, in quantum theory, by the optical coupling between two quantum states through the oscillator strength of the associated transition [46].

Within Lorentz model, the expression of the complex dielectric constant that describes the optical response of a set of harmonic and damped oscillators is given by [51, 54]:

$$\varepsilon(\omega) = 1 + \frac{e^2}{m\varepsilon_0}\sum_{k,l}\frac{N_{kl}}{\omega_{kl}^2-\omega^2-2i\omega\eta_{kl}} \qquad (7)$$

N_{kl} is the density of the electrons involved in the resonant transition ω_{kl}.

η_{kl} is the damping parameter correlated to the life time of the transition.

The effective masse was taken from literature data, $m = 0{,}2\ m_0$ [55].

It is well known that for ε–GaSe the direct and indirect band gaps are very close to each other. This is the subject of controversy in the literature regarding the nature of the fundamental gap. It is then worthy to take into account of this in the modeling. Thus, in equation 7, *k* stands for the VB states (P_z, P_x and P_y) all at Γ point and *l* for the CB direct states (S_d at Γ point) and for indirect ones (S_i at M point) as shown in Fig. 3.

Let us emphasize here that $\hbar\omega_{ks_i}$ is the energy of the absorbed photon which is different from the energy of the $E_k \rightarrow E_{s_i}$ indirect transition that, besides, involves either an absorption or an emission of an optical phonon: $E_{kS_i} = E_{s_i} - E_k = \hbar\omega_{ks_i} \pm \hbar\omega_{LO}$.

The imaginary part of the complex dielectric constant is derived from equation 7. Its expression is as follows:

$$\varepsilon_{Img}(\omega) = \frac{e^2}{m\varepsilon_0}\sum_{k,l}\frac{2N_{kl}\omega\eta_{kl}}{(\omega_{kl}^2-\omega^2)^2+4\omega^2{\eta_{kl}}^2} \qquad (8)$$

3.2.2 Fitting procedure and band structure features

Expression 8 allows the modeling of ε_{img}, of Fig.6, which has been accurately determined from both experiment and numerical procedure (as explained in the previous section). For a given resonance

(fixed k and l indices) there are 3 fitting parameters, $\omega_{kl}, N_{kl}\ and\ \eta_{kl}$. The steps that lead to the most accurate results consist on a fitting procedure comprising successively 3, 4 and 5 oscillators. The case of 3 oscillators takes into account only one kind of CB states without the possibility of knowing the corresponding nature. Increasing the number of the oscillators takes into account both indirect and direct CB states. The transitions considered are then ks_i, ks_d, where k takes successively the VB P_z, P_x and P_y states.

In Fig.7 we report the best fit for 3, 4 and 5 oscillator cases. Note the improvement in the adjustment to the experimental curve when the number of oscillators is increased.

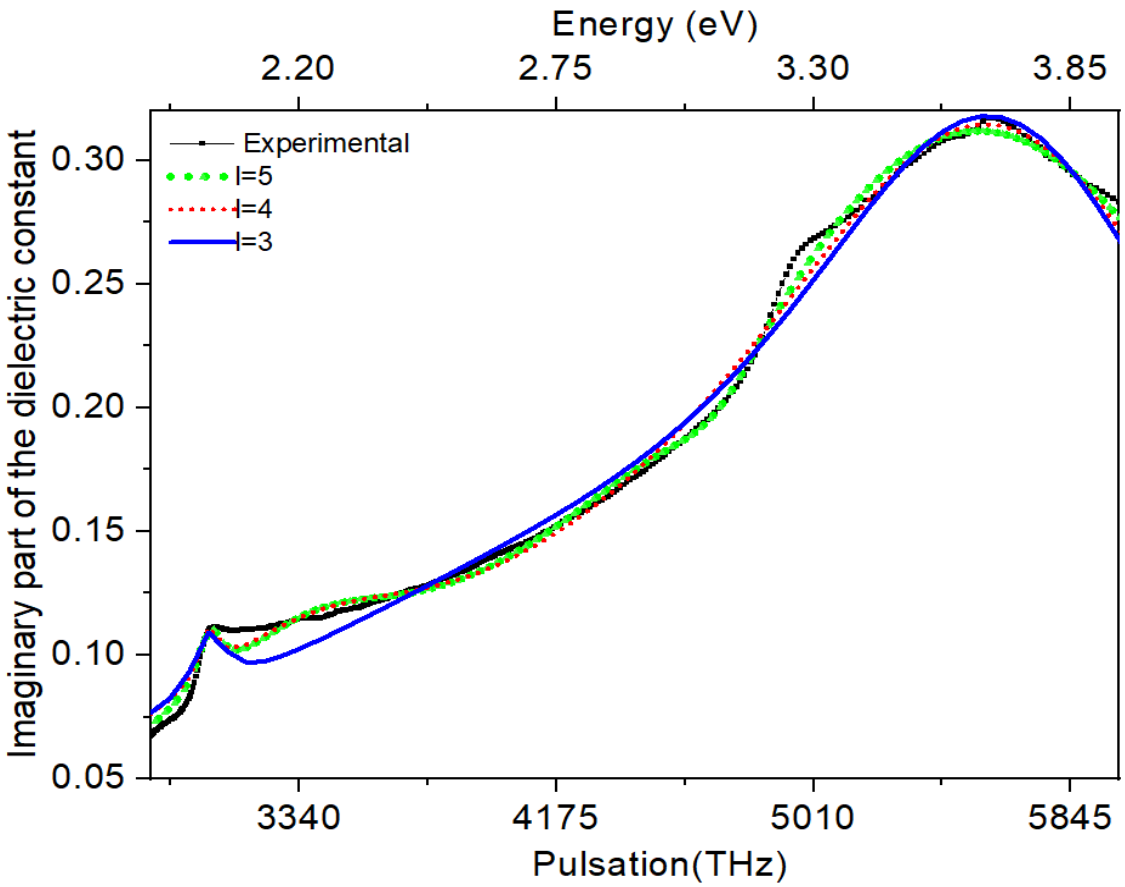

Fig. 7: Best fit of $\boldsymbol{\varepsilon_{img}}$ for 3, 4 and 5 oscillators. The adjustment is improved with the increase of the number of oscillators.

The position of each resonance, the density of electrons involved in the associated transition and the transition's lifetime ($\tau_{kl} = \eta_{kl}^{-1}$) are deduced from this best fit and grouped in Table 2.

Table2: The characteristics of the resonances observed in the transmittance and reflectance spectra of the GaSe sample. *k* represents the VB states (P_z, P_x and P_y) and *l* the CB states (S_d and S_i).

Transition	$\boldsymbol{P_zS_i}$	$\boldsymbol{P_zS_d}$	$\boldsymbol{P_xS_i}$	$\boldsymbol{P_xS_d}$	$\boldsymbol{P_yS}$
Nature of the transition	Indirect gap The fundamental gap	Direct gap	Indirect	Direct	Undetermined
$\hbar\boldsymbol{\omega_{kl}(eV)}$	2	2.2	3.1	3.3	3.7
$\boldsymbol{E_{kl}(eV)}$	1.97	2.2	3.07	3.3	Undetermined
$\boldsymbol{N_{kl}(10^{18}\,cm^{-3})}$	0.35	9	1.08	65.7	186
$\boldsymbol{\tau_{kl}(fs)}$	24	1.96	1.90	0.59	1

The values of the energy positions of the resonances are determined with great precision by the modeling procedure. In particular, the indirect and direct band gaps energies determined such a way are more precise than those which we had previously determined by a more approximate method based on Tauc's linearization [12].The values reported in Table 2 can then be considered as experimental values that should be compared with those determined from other kind of experiments and with those determined by first principles calculations for a better understanding of the singularities of ε–GaSe band structure.

From Table 2 we notice that the density of electrons involved in the lowest energy resonance, at 2 eV, and hence the associated oscillator strength, is much lower than that of the next closer resonance, at 2.2 eV ($N_{P_zS_i} < N_{P_zS_d}$). At the same time their lifetimes are such that $\tau_{P_zS_i} > \tau_{P_zS_d}$. Both of this findings support the fact that the fundamental gap of ε–GaSe (corresponding to the lowest energy transition) is of indirect nature. Its value can then be estimated, by considering the value of the LO phonon energy of about 30meV [56,57], as follows:

$$E_g^i = E_{P_zS_i} = E_{S_i} - E_{P_z} = \hbar\omega_{P_zS_i} - \hbar\omega_{LO} = 1.970\ eV.$$

Here we considered the most probable process, for low temperatures and even close to room temperature, in an indirect transition which consists of an emission of an optical phonon [51].

In fact, the parameters deduced for the two following transitions show that it is P_xS_i which is of an indirect nature whereas P_xS_d is of a direct nature, since $N_{P_xS_i} < N_{P_xS_d}$ and $\tau_{P_zS_i} > \tau_{P_zS_d}$. This confirms the previous assertion concerning the band gap nature.

However, we were not able to add a sixth oscillator to the modeling to decide on the nature of the last transition associated with the VB P_y, because the fitting procedure diverges.

The transitions lifetimes, that are the inverse of the corresponding damping parameters, are ranging between 0.6 *fs* and 24 *fs* as a consequence of the large gaps and the strong densities of carriers involved in the transitions. These values agree well with those reported, for ε-GaSe, by Qasrawi and Abdallah [58] and those that can be deduced from the damping parameters determined by Adachi and Shindo [48].

On another hand, our results obtained from a more precise procedure, when compared to the approximate use of Tauc's method, confirm a large indirect- direct band gaps separation in our sample. The energy difference between the two gaps reaches 230 meV which is significantly high compared to experimental values reported in the literature for unstrained GaSe crystals [13,28,57,59]. The highest value in unstrained layered GaSe, of about 130 meV, is reported by Sporken et al [28] using k-resolved inverse photoemission spectroscopy (KRISPES) measurements. On the other hand, the strong anisotropic nature of this quasi-2D material makes the layered crystals of GaSe very sensitive to strain [29,60].Gauthier et al [29] measured a separation of about 250 meV between the two gaps for layered crystals of GaSe under a hydrostatic pressure of 2 GPa. In our case, the large gaps separation is attributed to the strain that may result from the sample's bending that would take place following the exfoliation on the tape [12].

4. Conclusion

Complementary optical transmittance (T_{meas}) and reflectance (R_{meas}) measurements were carried out at room temperature on exfoliated GaSe multilayered crystal. There appear clear features related to strong absorptions from critical points of the Brillouin zone. The corresponding resonances at and far above the energy edge of the band gap have the same positions in both spectra.

The simultaneous measure of T_{meas} and R_{meas} enables a systematic and accurate determination of optical constants. Using this procedure, the absorption and reflection coefficients are accurately calculated in a wavelength range including transparent and absorbing regions for our exfoliated ε–GaSe sample. As a first consequence, its real refractive index is determined for the energy range 1.8 eV – 4 eV with values between 2.8 and 3.3 and strong peaks above the band gap corresponding to resonances at 3.2 eV and 3.7 eV. Then, the related complex refractive index and complex dielectric constant are both determined for any wavelength of the considered range. The modeling of the imaginary part, ε_{img}, of the complex dielectric constant within Lorentz model, permitted an accurate determination of each resonance's characteristics. The best fit of ε_{img} was obtained by

increasing the number of oscillators from 3 to 5, in agreement with the nature of the GaSe band structure which consists of 3 splited VB maxima, all at Γ point, and 2 CB minima at Γ and M points. These two CB minima are energetically very close in GaSe, which makes it difficult to assign the fundamental band gap. The adjusted parameters values, particularly of the density of electrons involved in each transition as well as of the corresponding lifetime, clearly show the indirect nature of the GaSe fundamental band gap. The indirect and direct band gaps values are respectively 1.97 eV and 2.2 eV. The large separation between the two gaps, of about 230 meV, reveals that sample is strained. The strain probably results from the bending following the exfoliation on the tape.

The approach considered in the present study, which is necessarily based on two complementary optical measurements and then on the exact calculation of both the absorption and the reflection coefficients is a good means for a precise determination of the optical parameters of non transparent materials.

References

[1] T. J. Bastow, I. D. Campbell, H. J. Whitfield, Solid State Commun. 39 (1981) 307.

[2] Z. He, J. Guo, S. Li, Z. Lei, L. Lin, Y. Ke, W. Jie, T. Gong, Y. Lin, T. Cheng, W. Huang, X. Zhang , Adv. Mater. Interfaces 7 (2020) 2070050.

[3] A. Abderrahmane, P. Jung, N. Kim, P. Ju Ko, A. Sandhu, Opt. Mater. Expr. 7 (2017) 587.

[4] P. Hu, Z. Wen, L. Wang, P. Tan, K. Xiao, ACS Nano. 6 (2012) 5988.

[5] N. Curreli, M. Serri, M. I. Zappia, D. Spirito, G. Bianca, J. Buha, L. Najafi, Z. Sofer, R. Krahne, V. Pellegrini, F. Bonaccorso Adv. Electron. Mater. 7 (2021) 2001080-1.

[6] A. S. Kumar, M. Wang, Y. Li, R. Fujita, X. P. A. Gao, ACS Appl. Mater. Interfaces 12 (2020) 46854.

[7] H. Tao, Q. Fun, T. Ma, S. Liu, H. Gysling, J. Texter, F. Guo, Z. Sun, Prog. Mater. Sci. 111 (2020) 100637.

[8] H. Ertap, Opt. Mater. 83 (2018) 99.

[9] A. Karaty, Opt. Laser Technol 111 (2019) 6.

[10] V.V. Zalamai, I.G. Stamov, N.N. Syrbu, Mater. Today Commun. 27 (2021) 102355.

[11] Y. Wu, H.-R. Fuh, D. Zhang, C.O. Coileain, H. Xu, J. Cho, M. Choi, B.S. Chun, X. Jiang, M. Abid, M. Abid, H. Liu, J. J. Wang, I.V. Shvets, C.-R. Chang, H.-C. Wu, Nano Energy 32 (2017) 157.

[12] A. Bassou , A. Rajira , M. El-Hattab , J. El Haskouri , S. M. Mascaros , A. Almaggoussi, A.Abounadi, Micro and Nanostructures 163 (2022) 107152 .

[13] L. Huang, Z. Chen, J. Li, RSC Adv. 5 (2015) 5788.

[14] Y. Ma, Y. Dai, M. Guo, L. Yu, B. Huang, Phys. Chem. Chem. Phys. 15 (2013) 7098.

[15] D. Rybkovskiy, N. Arutyunyan, A. Orekhov, I. Gromchenko, I.Vorobiev, A. Osadchy, E.Y. Salaev, T. Baykara, K. Allakhverdiev, E. Obraztsova, Phys. Rev. B 84 (2011) 085314.

[16] S. Lei, L. Ge, Z. Liu, S. Najmaei, G. Shi, G. You, J. Lou, R. Vajtai, P. M. Ajayan, Nano Lett.13 (2013) 2777.

[17] C. Wang, S. Yang, H. Zhang, L. Du, L. Wang, F. Yang, X. Zhang, Q. Liu, Front. Phys. 11 (2016) 116802.

[18] H. Ertap, Opt. Mater. 83 (2018) 99.

[19] Z. Wang, X. Wei, Y. Huang, J. Zhang, J. Yang, Mater. Sci. Semicond. Process. 159 (2023) 107393.

[20] X. Li, A. Bao, X. Guo, S. Ye, M. Chen, S. Hou, X. Ma, Appl. Surf. Sci. 618 (2023) 156544.

[21] D. Ghoneim, F.M. Hafez, S.N. El-Sayed, N.A. Mohsen, A.M.A. Mahmoud, IJRRAS 12 (2012) 56300721.

[22] M. Kępińska , M. Nowak , P. Duka , B. Kauch , Thin Solid Films 517 (2009) 3792.

[23] Y. Chen, Y. Sun, X. Dai, B. Zhang, Z. Ye, M. Wang, H. Wu, Thin Solid Films 592 (2015) 195.

[24] F.A. Garcés, N. Budini, R.D. Arce, J.A. Schmidt, Thin Solid Films 574 (2015) 162.

[25] R. Muydinov, A. Steigert, S. Schonau, F. Ruske, R. Kraehnert, B. Eckhardt, I. Lauermann, B. Szyszka, Thin Solid Films 590 (2015) 177.

[26] Y. Wang, A. Capretti, L.D. Negro, Opt. Mater. Express 5 (2015) 2415.

[27] J.I. Pankove, Optical Processes in Semiconductors, Dover, New York (1975).

[28] R. Sporken, R. Hafsi, F. Coletti, J.M. Debever, P.A. Thiry, A. Chevy, Phys. Rev. B49 (1994) 11093.

[29] M. Gauthier, A. Polian, J.M. Besson, A. Chevy, Phys. Rev. B 40 (1989) 3837.

[30] N.C. Fernelius Prog. Crystal Growth and Charact. 28 (1994) 275.

[31] F. Bassani, G. Pastori Parravicini, Il nuovo Cimento B 50 (1967) 95.

[32] J. Guo, J. Xie, D. Li, G. Yang, F. Chen, C. Wang, L. Zhang, Y. M. Andreev, K.A. Kokh, G.V. Lanskii, V.A. Svetlichnyi, Light: Science and Applications 4 (2015) 2047.

[33] F.I. Mustafa, S. Gupta, N. Goyal, S.K. Tripathi, Phys. Stat. Solidi C 6 (2009) S135.

[34] G.A. Akhundov, N.A. Gasanova, M.A. Nizametdinova , Phys. Stat. Sol. 15 (1966) K109.

[35] Web site: www.hq2d.com

[36] A. Bassou, A. Rajira, A. El Kanouny, A. Abounadi, J. El Haskouri, A. Almaggoussi, Mater. Today: Proc. 37 (2020) 3789-3792.

[37] G. Tse and D. Yu , Nanoelectron. and Optoelectron.11 (2016) 551.

[38] Y. Tang, W. Xie, K.C. Mandal, J.A. Mc Guire, C.W. Lai, Phys. Rev. B 91 (2015) 1.

[39] Y. Tang, W. Xie, K.C. Mandal, J.A. Mc Guire, C.W. Lai, J. Appl. Phys. 118 (2015) 113103.

[40] S.G. Choi, D.H. Levi, C.M. Tomas, V.M. Sanjosé, J. Appl. Phys. 106 (2009) 053517.

[41] F.K. Shan, G.X. Liu, W.J. Lee, G. H. Lee, I.S. Kim, B.C. Shin, J. Appl. Phys. 98 (2005) 023504.

[42] A.S. Hassanien, A.A. Akl , Physica B: Physics of Condens. Matter. 576 (2020) 411718.

[43] A.S. Hassanien, A.A. Akl, J. Alloys Compd. 648 (2015) 280.

[44] F.A. Jenkins and H.E. White, Fundamentals of Optics, 4th ed.McGraw-Hill Higher Education, New York,(1976).

[45] D.C.Look, J.H. Leach J. Vac. Sci. Technol. B 34 (2016) 04J105-1.

[46] S.K. Gautam, R.G. Singh, V.V. Siva Kumar, F. Singh, Solid. State Commun. 218 (2015) 20.

[47] A.S. Hassanien J. Non Cryst. Solids. 586 (2022) 121563.

[48] S. Adachi and Y. Shindo, J. Appl. Phys. **76** (1992) 514.

[49] R. L. Toullec, N. Piccioli, M. Mejatty, M. Balkanski, Nuovo Cimento B 38 (1977) 159.

[50] K. R. Allakhverdiev, T. Baykara, A. Kulibekov Gulubayov, A. A. Kaya, J. Goldstein, N. Fernelius, S. Hanna and Z. Salaeva, J. Appl. Phys. 98 (2005) 093515.

[51] F. Wooten, Optical Properties of Solids, Academic Press, New York (1972).

[52] K. K. Ahmed , S. B. Aziz, R. T. Abdulwahid, S. A. Hussen , M.A. Brza Opt. Mater. 134 (2022) 113112.

[53] A. H.A. Darwesh , S. B.Aziz , S. A. Hussen Opt. Mater 133 (2022) 113007.

[54] M. Dresselhaus , G. Dresselhaus, S.B. Cronin, A.G.S. Filho, Solid. State Properties, From Bulk to Nano, Springer, Berlin (2018).

[55] O. Madelung, Semiconductors Data handbook, Marburg: Springer Science &Business Media, Berlin (2012).

[56] V. Capozzi, S. Caneppele, M. Montagna, F. Lévy, Phys. Stat. Solidi (b) 129 (1985) 247.

[57] K. Allakhverdiev, T. Baykara, S. Ellialtioglu, F. Hashimzade , D. Huseinova, K. Kawamura, A.A. Kaya, A.M. Kulibekov (Gulubayov), S. Onari, Materials Research Bulletin 41 (2006) 751.

[58] A.F. Qasrawi, Maisam M.A. Abdallah Optik 168 (2018) 481.

[59] A.V. Kosobusky, S. Yu. Sarkisov, V.N. Brudnyi, J. Phys. Chem. Solids 9 (2013) 1240.

[60] Y. Wu, H.-R. Fuh, D. Zhang, C. O. Coileain, H. Xu, J. Cho, M. Choi, B. S. Chun, X. Jiang, M. Abid, M. Abid, H. Liu, J. J. Wang, I. V. Shvets, C.-R. Chang, H.-C. Wu, Nano Energy 32 (2017) 157.